The Design of Rice Powder Production Vessel and the Pulverization of the Rice Using Numerical Simulation

Manabu SHIBUTA[1], Hideki HAMASHIMA[2], Shigeru ITOH[3]
[1]Graduate School of Science and Technology, Kumamoto Univ.
2-39-1 Kurokami, Kumamoto 860-8555, Japan
manabu@shock.smrc.kumamoto-u.ac.jp
[2]Kumamoto Industrial Research Institute.
3-11-38 Higashimachi, Kumamoto 862-0901, Japan
hamashima@kmt-iri.go.jp
[3]Okinawa National College of Technology.
905 Henoko, Nago City, Okinawa 905-2192, Japan
itoh_lab@okinawa-ct.ac.jp

ABSTRACT

In recent years, the food self-support rate of Japan is 40%, and this value is the lowest level of major advanced country. The stable supply of food is a big subject that Japan has. Therefore, rice powder attracts attention for improvement of the food self-support rate in Japan.

Previously, the rice powder is produced by two methods. One is dry type, and the other is wet type. However, these systems have a fault of the heat damage of the starch and the consumption of a large quantity of water. In our laboratory, as solution of those problems, production of the rice powder by using the underwater shock wave is considered.

Shock wave is the pressure wave which is over velocity of sound by discharging high energy in short time. Propagating shock wave in water is the underwater shock wave. This food processing using an underwater shock wave has little influence of heat and its processing time is very short, preventing the loss of nutrients.

In this research optical observation experiment and the numerical simulation were performed using trial vessel, in order to understand the behavior of the underwater shock wave in the development of the rice powder production vessel using an underwater shock wave at the factory. In addition, in order to understand the rice powder production and to develop it, the numerical simulation about pulverization of rice is performed. By this method, the pressure which takes for rice at the time of pulverization, and its pulverization phenomenon are solved. Analysis soft LS-DYNA was used for these numerical simulations.

The comparative study of the experiment and the numerical simulation was investigated. The behavior of the shock wave in the device and transformation of rice were able to be clarified.

1. INTRODUCTION

Various processing methods of using shock waves generated by explosive and electric power have been studied and developed. It is well established that shock wave pressure propagates on a large range and duration of pulse can be long, depending on the processing techniques.

Using water as the propagation medium, the influence of thermal effect can be minimized. Rice powder is produced using this advantage.

In this research, the purpose is the utilization of the rice powder manufacture using the shock wave. Therefore, it needs to understand the following points. At first, the device with the optimal form and strength to utilize the shock wave for the maximum is designed. And next, in order to produce rice powder efficiently, it is necessary to know the destructive phenomenon of rice and the influence of the shock wave on rice. However, a cost depends on an experiment, and the observation of the phenomenon is difficult. Therefore we used numerical simulation. In design of the device, a high speed camera was used for optical observation of shock waves. And numerical simulation was performed to investigate the validity of data, and these results were compared with experimental results. [1]

Moreover, in order to know what kind of influence the observed shock wave will have on food processing, influence evaluation of the shock wave by the form of a device was performed. The simulation method using SPH is proposed about the pulverization phenomenon of rice. About a pulverization phenomenon of rice, two kinds of simulation method ware proposed.

2. THE DESIGN OF THE SHOCK WAVE PROCESSING DEVICE

2.1. EXPERIMENTAL METHOD AND NUMERICAL SIMULATION METHOD

2.1.1. Optical observation method and Experimental device

The optical observation that uses the shadowgraph method [2] was used to evaluate the shock wave propagating. The shadowgraph system used in this study is shown in Fig.1. This system uses a technique, also called direct projective technique, in which the shadow of the light observed and projected by density change on a screen. The shadowgraph method used for visualization of a shock wave or the motion of a wave is a classical technique.

The shadowgraph system and a high-speed video camera (HPV-1:Shimadzu Corp.) were used to observe the underwater shock wave. The velocity of a shock wave is obtained by taking a framing photography using the shadowgraph method. The schematic illustration of an optical observation for the framing photography is shown in Fig.2.

An experimental device is a rectangular container. The observation side of the device is PMMA, the side of the device is aluminum and the upper surface and the bottom of the device are PMMA. This container is separated into two parts by a phosphor bronze plate. 0ne part is the shock wave generating container and the other is the food processing container. In order to generate a shock wave in the upper part of the device, the No.6 electric detonator (made by Kayaku Japan corporation) is set.

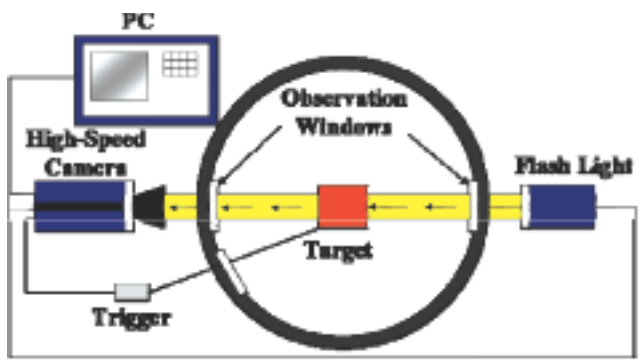

Figure 1 Shadowgraph system for optical observation

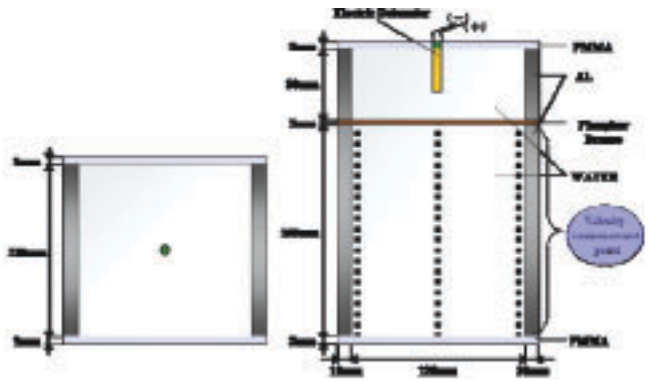

Figure 2 Schematic illustration of an optical observation for the framing photography

The inner volume of the shock wave generating container is 120mm × 120mm × 50mm and the size of the food processing container is 120mm × 120mm × 150mm. Water is poured into each.

2.1.2. Numerical Simulation Condition

The phenomenon for an explosion and the propagation of shock wave in the device are evaluated by means of LS-DYNA. Fig.3 shows to the numerical simulation model of the device. This simulation model is two dimension model of one mesh in depth. And calculation method is used Lagrangian and Eulerian [3,4]. The number of elements is 29820 (=213 × 140 × 1).

High explosives SEP (made by Kayaku Japan corporation, detonation velocity about 6,800m/s, density 1310 kg/m^3) is detonated by using Initial detonation. Because the structure of the electric detonator is complex, SEP to which the parameter value is known instead of the electric detonator is used. The power of explosive SEP is coordinated to become at the same level as an electric detonator. We applied the constrained condition for the z axis so that a translational and rotational motion can not happen when explosion is occurred in explosive container.

The various conditions used for this numerical simulation are shown below.

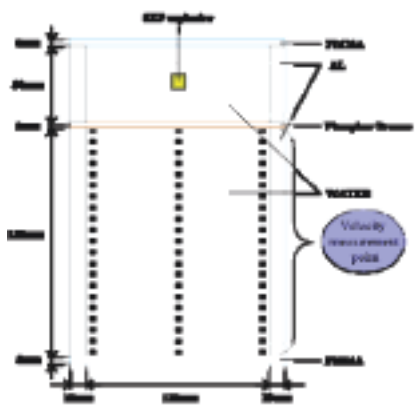

Figure 3 Simulation model of the device

- Explosive SEP
  Jones-Wilkins-Lee (JWL) equation of state [5,6] for the explosive SEP is used. This equation is well used for the numerical simulation accompanied by a detonation phenomenon. JWL parameters are given in Table 1. Expression of JWL equation of state is described as follows:

$$P = A\left[1-\frac{\omega}{VR_1}\right]\exp(-R_1V)+B\left[1-\frac{\omega}{VR_2}\right]\exp(-R_2V)+\frac{\omega E}{V} \tag{1}$$

  $V = \rho_0$ (Initial density of an explosive) /ρ (Density of detonation gas), P is Pressure, E is Specific internal energy, A, B, R_1, R_2, ω are JWL parameters.

Table 1 Parameter of JWL equation of state of SEP

	A [GPa]	**B [GPa]**	R_1	R_2	ω
SEP	364	2.31	4.3	1	0.28

- WATER
  We applied GRUNEISEN equation of state and NULL for the material parameter of water.
  - GRUNEISEN equation of state
    This equation of state with cubic shock velocity-particle velocity defines pressure for compressed material as

$$p = \frac{\rho_0 C^2\mu\left[1+\left(1-\frac{\gamma_0}{2}\right)\mu-\frac{a}{2}\mu^2\right]}{\left[1-(S_1-1)\mu-S_2\frac{\mu^2}{\mu+1}-S_3\frac{\mu^3}{(\mu+1)^2}\right]^2}+(\gamma_0+a\mu)E \tag{2}$$

    C is the intercept of the v_s-v_p curve, S_1, S_2 and S_3 are the coefficients of the slope of the v_s-v_p curve, γ_0 is the Gruneisen gamma, a is the first order volume correction to γ_0, $\mu = \frac{\rho}{\rho_0}-1$ Gruneisen coefficients are given in Table 2.

Table 2 Parameter of Gruneisen equation of state of WATER

	c	S_1	S_2	S_3	γ_0	a	E
WATER	1647.0	1.921	−0.096	0.0	0.35	0.0	2.895e+05

- NULL
  This material allows equations of state to be considered without computing deviatoric stress. Optionally, a viscosity can be defined. Also, erosion in tension and compression is possible. Material parameter of WATER for NULL is given in Table 3.
- Aluminum alloy
  We applied SIMPLIFIED JOHNSON COOK for the material parameter of Aluminum alloy. This Johnson cook strain sensitive plasticity is used for problems where the strain rates vary over a large range. In this simplified model, thermal effects and damage are ignored. The value of AL6082-T6 is used as a value of the aluminum alloy

Table 3 NULL parameter of WATER

	RO	PC	MU	TEROD	CEROD	YM	PR
WATER	998.21002	0.0	8.684e-04	0.0	0.0	0.0	0.0

RO : Mass density PC : Pressure cutoff MU : Dynamic viscosity coefficient

TEROD,CEROD : Relative volume YM : Young's modulus PR : Poissin's ratio

this time. Material parameter of Aluminum ally for SIMPLIFIED JOHNSON COOK are given in Table 4. Expression of SIMPLIFIED JOHNSON COOK is described as follows:

$$\sigma_y = \left(A + B\bar{\varepsilon}^{p^n} \right)\left(1 + c\ln \dot{\varepsilon}^*\right) \tag{3}$$

A, B, C and *n* are constants. $\bar{\varepsilon}^p$ =effective plastic strain. $\dot{\varepsilon}^* = \frac{\dot{\bar{\varepsilon}}}{\dot{\varepsilon}_0}$ effective strain rate for $\dot{\varepsilon}_0 = 1s^{-1}$

Table 4 SIMPLIFIED JOHNSON COOK parameters of AL6082-T6

	A	*B*	*C*	*n*
AL6082-T6	4.285e+08	3.277e+08	0.00747	1.008

- Phosphor bronze, PMMA
  We applied PLASTIC KINEMATIC for the material parameter of Phosphor bronze and PMMA. This model is suited to model isotropic and kinematic hardening plasticity with option of including rate effects. Material parameter of Phosphor bronze and PMMA for PLASTIC KINEMATIC are given in Table 5.

Table 5 Material parameters of phosphor bronze and PMMA

Phosphor	**RO**	**E**	**PR**	**SIGY**	**ETAN**	**BETA**
bronze	8890	1.2e+11	0.38	6.0e+08	0.0	0.0
	SRC	SRP	FS	VP		
	0.0	0.0	0.0	0.0		
PMMA	RO	E	PR	SIGY	ETAN	BETA
	1180	3.4e+09	0.3	7.0e+07	0.0	0.0
	SRC	SRP	FS	VP		
	0.0	0.0	0.0	0.0		

RO : Mass density E : Young's modulus PR : Poissin's ratio ETAN : Tangent modulus

BETA : Hardening parameter SRC : Strain rate parameter SRP : Strain rate parameter

FS : Failure strain eroding elements VP : Formulation for rate effects

- Coupling
  In this research, CONSTRAINED LAGRANGE IN SOLID was used in order to perform coupling of water and metal material in LS-DYNA. This command provides the coupling mechanism for modeling Fluid-Structure Interaction (FSI). The structure can be constructed from Lagrangian shell and/or solid entities. The multi-material fluids are modeled by ALE formulation.

  Other condition of numerical simulation is shown in Table 6.

Table 6 Condition of Numerical calculation analysis

Code		**LS-DYNA**
Calculation method	Lagrangian & Eulerian	
Equation of state	SEP	JWL
	WATER	GRUNEISEN
MAT	WATER	NULL
	Aluminum alloy	SIMPLIFIED JOHNSO COOK
	PMMA	PLASTIC KINEMATIC
	Phosphor Bronze	PLASTIC KINEMATIC
Mesh size	1.0 × 1.0 × 1.0 mm	
Element	29820 (=213 × 140 × 1)	
Initial condition	INITIAL DETONATION	
Contact condition	ERODING SURFACE TO SURFACE	
Coupling condition	CONSTRAINED LAGRANGE IN SOLID	

2.2. THE COMPARISON OF EXPERIMENTAL RESULTS AND SIMULATION RESULTS [1]

The framing photographs showing the behavior of the shock wave which propagates the inside of a processing device were obtained by optical observation using the high-speed video camera. The framing photographs are shown in Fig.4. First, the shock wave with detonation velocity of No.6 electric detonator propagates into the water and the shock wave passes through the phosphor bronze plate at 5μs can be confirmed. The precursor shock wave generated by the shock wave propagated from the phosphor bronze plate to the aluminum sidewall can be confirmed at 20μs. It is understood that the precursor shock wave propagate from the phosphor bronze because the shock wave propagated from a lower wall before the shock wave reaches the upper wall. In the photograph of 35μs, the reflected wave that the shock wave that propagates by passing the phosphor bronze plate reflects to the sidewall was able to be observed. In addition, the height of the whole device is 213mm, but the distance from the phosphor bronze plate in the observation part is about 95mm at the maximum to observe the processing container part in the experiment.

The pressure distribution of the precursor shock wave and the shock wave passes through the phosphor bronze plate that obtained by numerical simulation is shown in Fig.5. These photographs show that Explosive SEP explodes and shock wave propagates. The precursor shock wave propagates from the aluminum sidewall into water. Fig.6 has changed the pressure representation at the time of 60μs compared with Fig.7. The reflected shock wave that the shock wave that propagates by passing the phosphor bronze plate reflects to the sidewall was able to be observed.

What measured the velocity of precursor shock wave, shock wave passes through the phosphor bronze plate (Henceforth, this is called Shock wave) and shock wave reflected in the side wall is shown in Fig.7, Fig.8, and Fig.9.

In these results, since there is the same tendency as an experiment and numerical analysis in each shock wave, it can be considered that this numerical analysis is effective as the evaluation method.

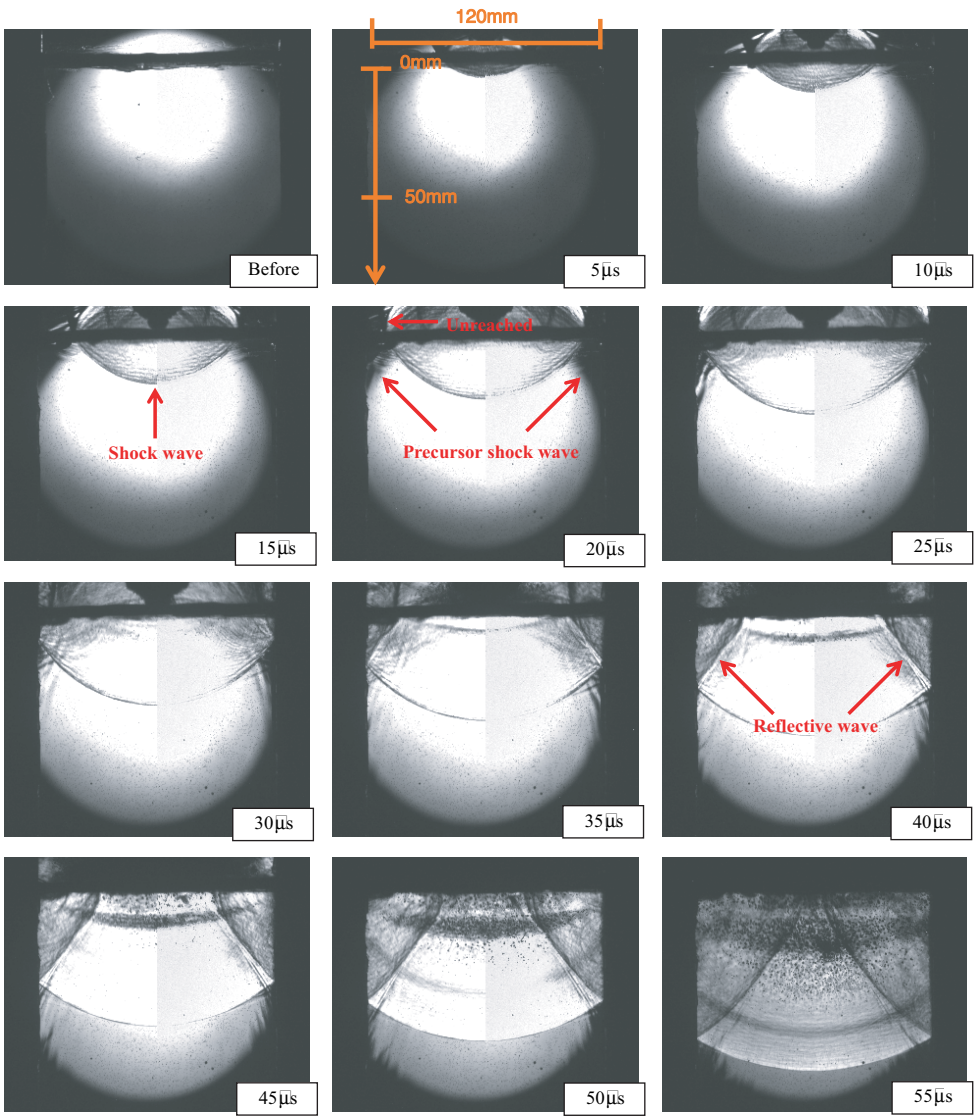

Figure 4 Framing photographs of underwater shock wave

Fig.6 Framing photographs of underwater shock wave

2.1.2. Evaluation of the device form

The optimal form of a device is considered, because effectiveness was shown in the device design using numerical simulation. In this case, numerical simulation is performed in order to investigate what kind of influence a shock wave has on food processing, and the device where the shock wave acts easily is designed.

In this paragraph, the numerical simulation shown in Fig.10, 11, 13, 15, 17 was performed. The pressure in Fig.10 and other figures is measured, and a result is shown in Fig.12, 14, 16, 18. Pressure was measured at a 30mm point from the phosphor bronze plate

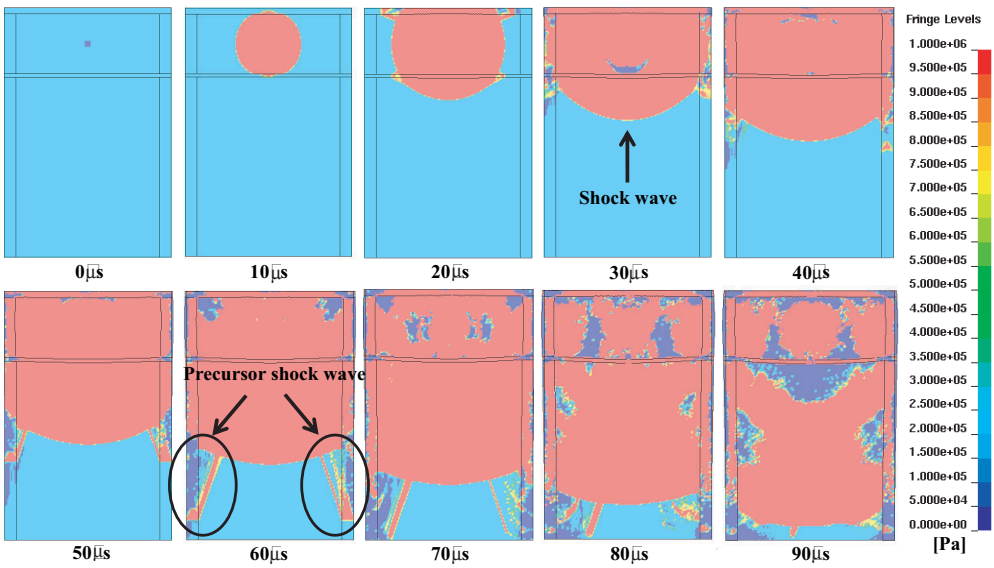

Figure 5 Calculated pressure contours under water (precursor shock wave and shock wave)

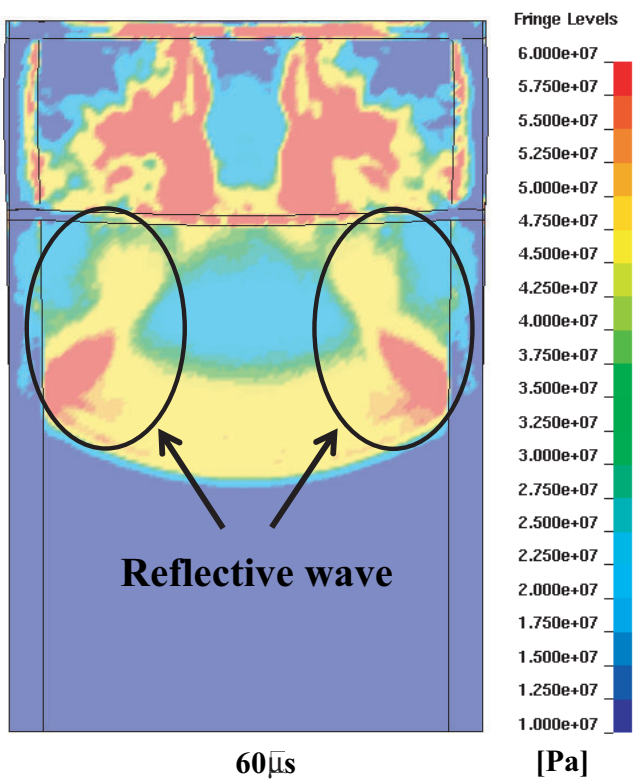

Figure 6 Calculated pressure contours under water (reflective wave)

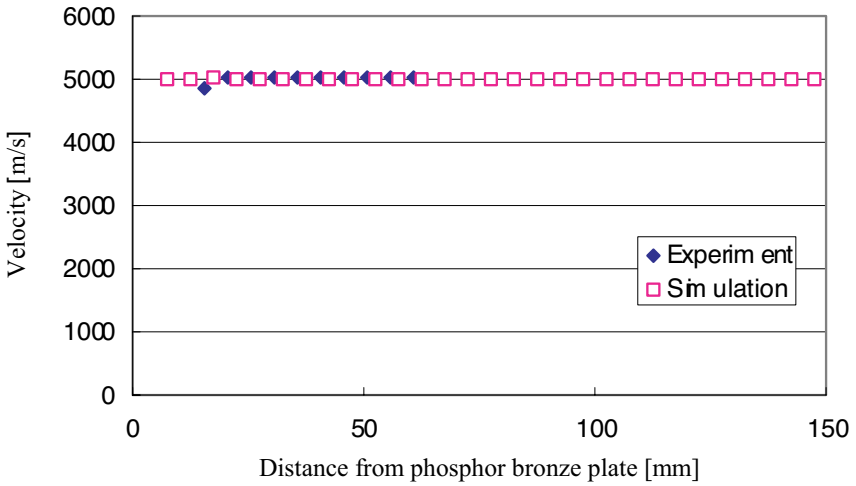

Figure 7 Comparison of velocity of precursor shock wave

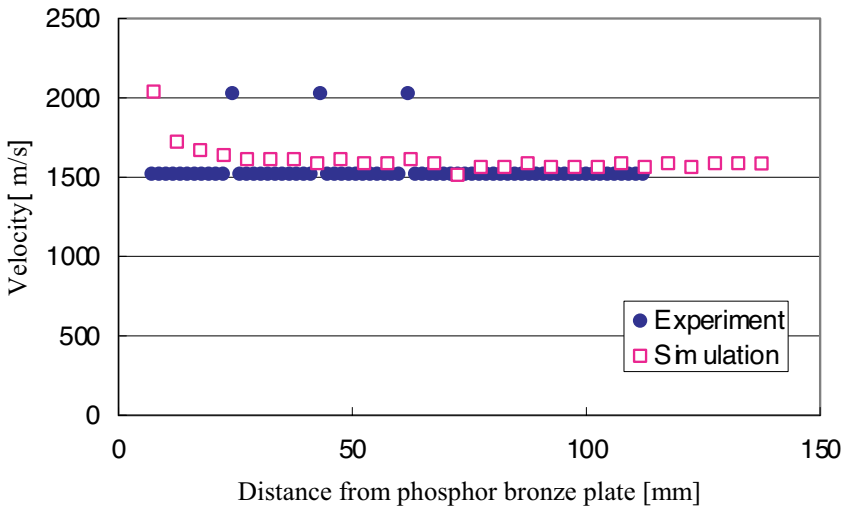

Figure 8 Comparison of velocity of shock wave

in the center of a processing container. This point is a place to put food. Moreover, all the results are compared and it is shown in Fig.19.

The figure is explained here. Fig.10 is the model that SEP detonates in underwater, in order to consider the validity of equipment. Fig.11 shows the same model as what was used in the experiment. Fig.13 is the model that the aluminum side wall of the food processing container of figure 11 was removed. In consideration of reflection on the boundary, the water part is larger than Fig.11. Furthermore, as for Fig.15, the aluminum side wall of a shock wave generating container is also removed. Fig.17 is the model which removed the phosphor bronze plate from the equipment used for the experiment.

Two peaks were observed by the pressure value in simulation. Each peak is called the first shock wave and the second shock wave. Each consideration is shown below.

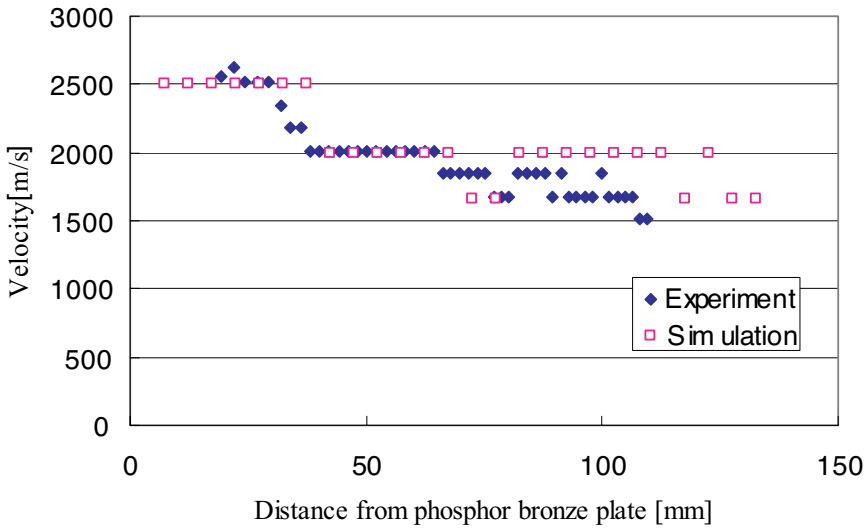

Figure 9 Comparison of velocity of reflective wave

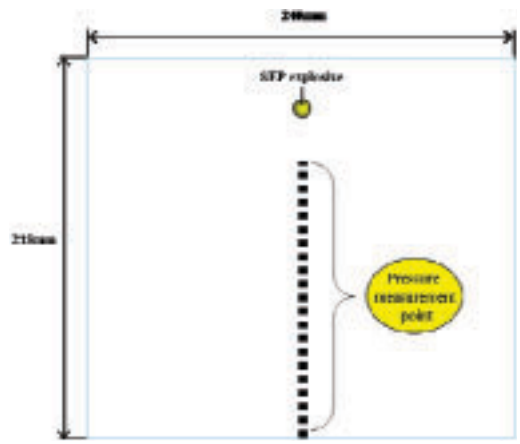

Figure 10 Simulation model of the only water

- The First Shock wave
  The first shock wave was observed in all results. This shock wave was generated when SEP detonated.

  The maximum pressure of the first shock wave in Fig. 10 is about 380 MPa. This value is about two times of Fig.12, 14, 16 and the same level in fig.18. In Fig.12, 14, 16, pressure became about half compared with the case of only water and the difference was in the time which measured pressure. It is thought that this is caused by attenuation of the pressure, when the shock wave passed the phosphor bronze plate which is a partition of a shock wave generating part and a food processing part. It is clear also from the result of Fig.18 that there is not phosphor bronze plate.
- The Second Shock wave

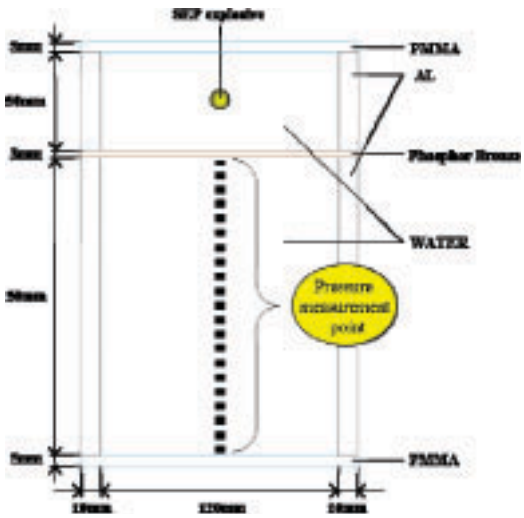

Figure 11 Simulation model of the experimental device

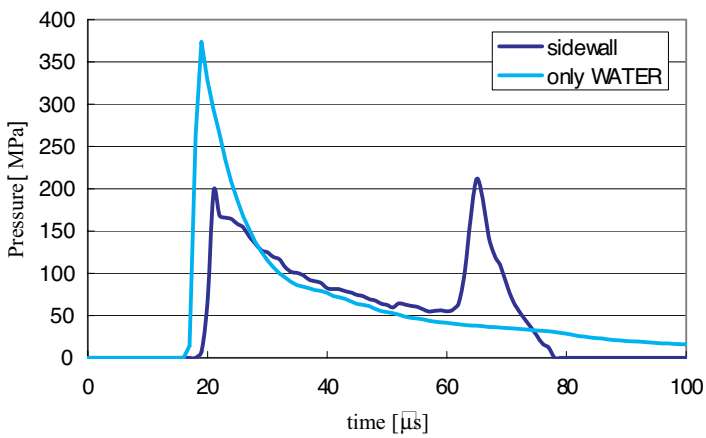

Figure 12 Comparison of experimental device and only water

The second shock wave was observed in all results except for Fig.16. It is thought that this shock wave observed the first shock wave reflected in the aluminum side wall (reflective shock wave). This is clear also from not observing the second shock wave in the model of Fig.10 and Fig.15 that is a model without the aluminum side wall.

The maximum pressure of the second shock wave is about 210 MPa in Fig.12, is about 320 MPa in Fig.14, and is about 100 MPa and in Fig.18. In Fig.12, it is thought that the first shock wave reflected in the aluminum side wall of a food processing part was observed. In Fig.14, it is thought that the shock wave reflected in the aluminum side wall of a shock wave generating part was observed. Also in Fig.12, since the minor change occurred in the attenuation tendency of pressure in about 70μs, it is thought that the shock wave reflected in the aluminum side wall of the generating part was observed. The reflective shock wave can be observed twice in Fig.18. In Fig.18, as the reason that the pressure of the second

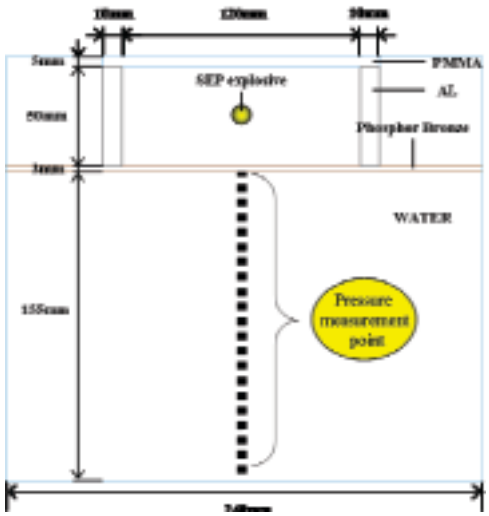

Figure 13 Simulation model of the device without the side wall

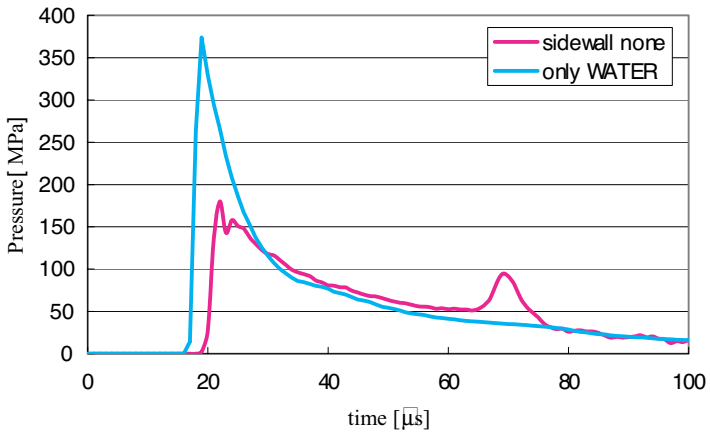

Figure 14 Comparison of nothing sidewall and only water

shock wave is big compared with other case, it is thought that there is no attenuation of pressure with the phosphor bronze plate, as well as the first shock wave.

It is effective to make a shock wave act many times, when performing food processing using a shock wave. Therefore it is thought that it is necessary to have the following form as a processor.

- The first shock wave spreads in a food processing part without decreasing as much as possible
- The second shock wave (reflective wave) acts on the food processing part efficiently by high pressure

Although the phosphor bronze plate was used in order to protect food from pollution of the water which can occur on the shock wave generating part, it is necessary to think about the necessity of the plate when considering the form of the device.

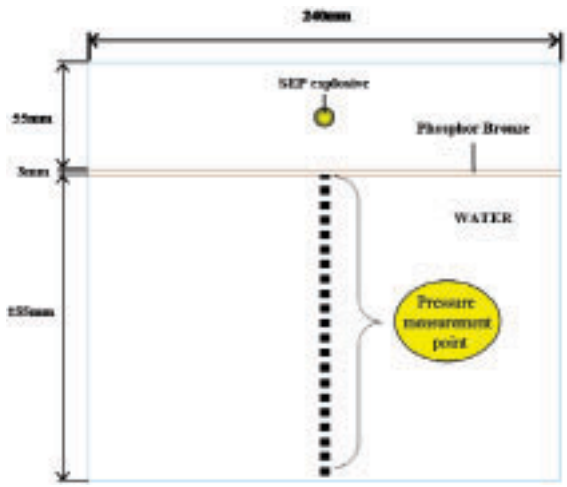

Figure 15 Simulation model of only the Phosphor Bronze Plate

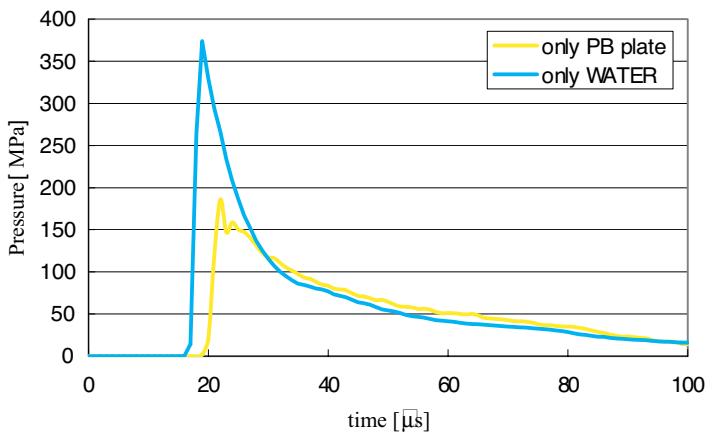

Figure 16 Comparison of only PB plate and only water

3. THE PROPOSAL OF THE TECHNIQUE IN REAPPEARANCE OF THE PULVERIZATION PHENOMENON OF RICE

Now, the numerical simulation of the pulverization phenomenon by the shock wave of rice is not known. Therefore it proposes using the numerical analysis using the following techniques as reappearance of the pulverization phenomenon of rice.

3.1. THE PULVERIZATION SIMULATION OF RICE (TYPE 1)

3.1.1. Numerical Simulation Condition of Type 1

Fig.20 shows the numerical simulation model of the rice. This simulation model is three dimensional model and depth is four meshes. And calculation method is used Lagrangian and Eulerian like 2.2.1. The number of elements is 45077.

SEP and WATER are the same as 2.2.1. Therefore only rice is described. The various conditions used for this numerical simulation are shown below.

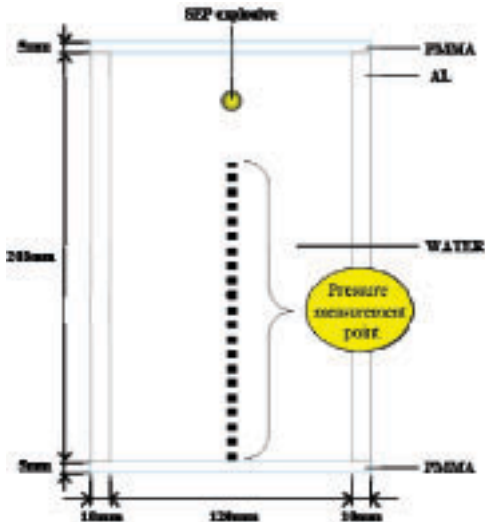

Figure 17 Simulation model of the device without the PB plate

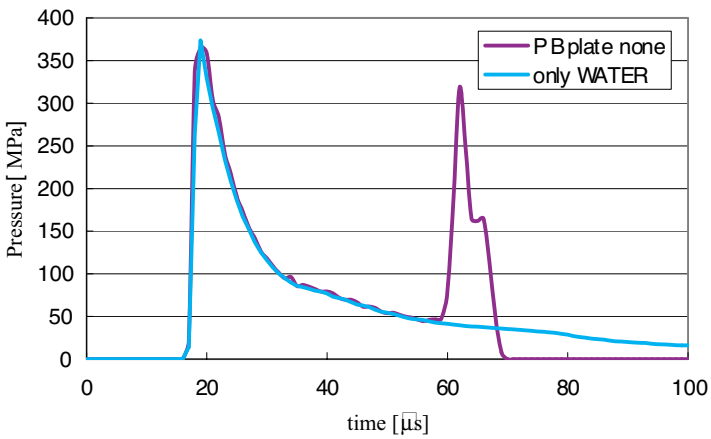

Figure 18 Comparison of nothing PB plate and only water

- Rice
  We applied GRUNEISEN equation of state and ELASTIC PLASTIC HYDRO for the material parameter of rice. Since GRUNEISEN is described in 2.2.1, only the parameter of rice is described to Table 7 and explanation describes only ELASTIC PLASTIC HYDRO. In addition, since the exact parameter of rice was unknown, the value of carbon was used.

Table 7 Parameter of Gruneisen equation of state of Rice

	c	S_1	S_2	S_3	γ_0	a	E
WATER	320.0	1.18	0.0	0.0	2.0	0.0	0.0

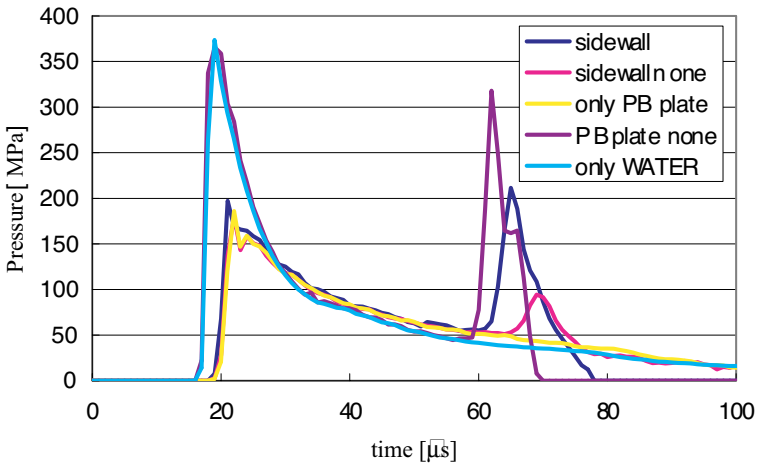

Figure 19 The pressure comparison of all results

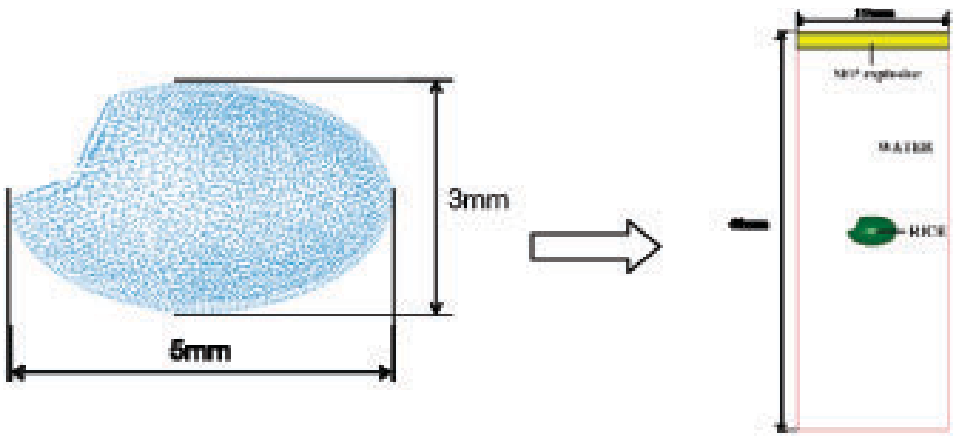

Figure 20 Numerical simulation model of the rice type 1

- ELASTIC PLASTIC HYDRO
  This material allows the modeling of an elastic-plastic hydrodynamic material. Material parameter of WATER for ELASTIC PLASTIC HYDRO is given in Table 8.

Table 8 ELASTIC PLASTIC HYDRO parameter of Rice

	RO	G	SIGY	EH	PC	FS
WATER	320.0	1.0e+10	4.0e+08	0.0	0.0	0.0

RO : Mass density G : Shear modulus SIGY : Yield stress
EH : Plastic hardening modulus PC : Pressure cutoff FS : Failure strain for erosion

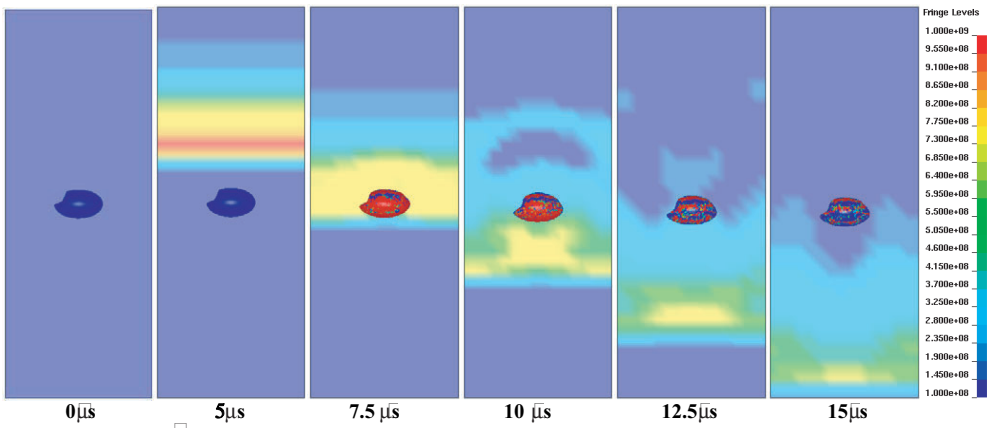

Figure 21 Pulverization Simulation of Rice (Type 1)

Other condition of numerical simulation is shown in Table 9.

Table 9 Condition of Numerical Simulation of Type1

Code	**LS-DYNA**	
Calculation method	Lagrangian & Eulerian	
Equation of state	SEP	JWL
	WATER & Rice	GRUNEISEN
MAT	WATER	NULL
	Rice	ELASTIC PLASTIC HYDRO
Mesh size	1.0 × 1.0 × 1.0 mm	
Element	45077	
Initial condition	INITIAL DETONATION	

3.1.2. Simulation Result of Type 1

Modification of rice was observed when a shock wave reached rice. However, it has not resulted in reappearance of pulverization of rice.

3.2. THE PULVERIZATION SIMULATION OF RICE (TYPE 2)

3.2.1. Numerical Simulation Condition of Type 2

Numerical simulation using SPH as another method for reappearing pulverization of rice was

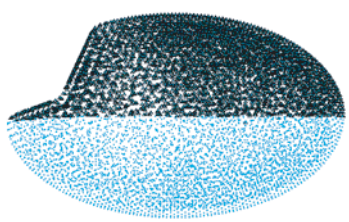

Figure 22 Numerical Simulation model of the Rice (Type 2)

performed. The simulation model is shown in Fig.22. In order to make it simple, an action of a shock wave is resembled by giving velocity to a surface upper half (black part). The number of elements is 42677.

The u_p is velocity given on the surface of rice. This velocity was obtained from the following formulas and values.

$$P = \rho U_s u_p \tag{4}$$

The velocity and each value are shown in Table 10. Each value obtained from Type1. This is the adjacent value of the shock wave incident on rice.

Table 10 Numerical value used for Simulation

P : pressure	ρ : density	U_s : shock wave velocity	u_p : particle velocity
670MPa	1000kg/m^3	1500m/s	450m/s

Other condition of numerical simulation is shown in Table 11.

Table 11 Condition of Numerical Simulation of Type2

Code	LS-DYNA	
Calculation method	SPH	
Equation of state	Rice	GRUNEISEN
MAT	Rice	ELASTIC PLASTIC HYDRO
Mesh size	0.1 × 0.1 × 0.1 mm	
Element	42677	
Initial condition	INITIAL VELOCITY	

3.2.2. Simulation Result of Type 2

The pulverization phenomenon of the rice reappeared by numerical simulation is shown in Fig. 23. A pulverization phenomenon by the repetition of contraction and expansion of rice was reproduced. Partial crush occurred. The same phenomenon is confirmed in the

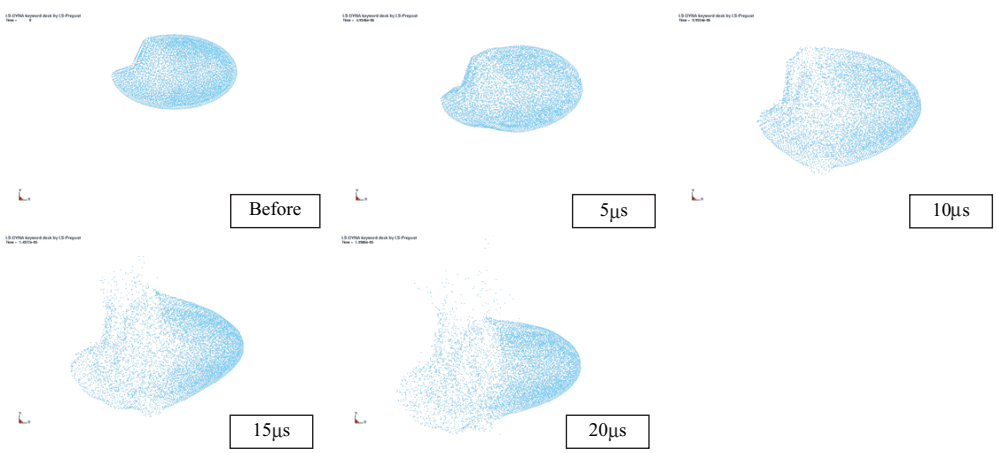

Figure 23 Pulverization Simulation of Rice (Type 2)

pulverization experiment of rice. For this reason, pulverization reappearance of the rice in this numerical simulation is considered to be one of the effective simulation techniques.

4. CONCLUSION

This research aimed at the design of the processing device of the rice and reappearing the pulverization of rice which used numerical analysis. It succeeded in the high-speed photography and numerical simulation of the three kinds of shock waves. From the comparison of these results, effectiveness was admitted in the device design by the numerical simulation.

In addition, the validity of the reflective shock wave in food processing and suitable device form were shown by simulation. In addition, the simplified pulverization process of rice was reproducible.

In future works, in order to explore more effective device form, exact simulation by three dimensions is realized. In addition, in the pulverization simulation of rice, it is required to obtain the exact parameter of rice.

REFERENCE

[1] M.Shibuta, H.Hamashima, S.Itoh, Numerical Simulation and Experiment for Underwater Shock Wave in Newly Designed Pressure Vessel, The International Journal of Multiphysics, Volume 4, Number 3, pp.259–271(2010)

[2] S.Itoh, Z.Liu, Y.Nadamitu, An Investigation on the Properties of Underwater Shock Waves Generated in Underwater Explosions of High Explosives, Journal of Pressure Vessel Technology, Vol.119, pp.498–502 (1997)

[3] J.O. Hallquist, “LS-DYNA Theoretical Manual”, Livermore Software Technology Corporation (2006).

[4] J.O. Hallquist, “LS-DYNA Keyword User’s Manual”, Livermore Software Technology Corporation (2007).

[5] J. W. Kury, H. C.Hornig, E. L. Lee, J. L. McDonnel, D. L. Ornellas, M.Finger, F. M. Strange and M. L. Wilkins, Metal Acceleration by Chemical Explosives, 4th Symposium on Detonation, A109–A120 (1965)

[6] E. L. Lee, M.Finger and W.Collins, JWL Equation of state Coefficients for High Explosives, Lawrence Livermore Laboratory, UCID-16189 (1973)